Endoglin and the immune system: immunomodulation and therapeutic opportunities for cancer

Schoonderwoerd, M.J.A.

6

Targeting endoglin expressing regulatory T cells in the tumor microenvironment enhances the effect of PD1 checkpoint inhibitor immunotherapy

CLIN CANCER RES. 2020 JUL

M.J.A. Schoonderwoerd[1], M.F.M Koops[1]*, R.A. Angela[1]*, B. Koolmoes[1], M. Toitou[1], M. Paauwe[1], M.C. Barnhoorn[1], Y. Liu[2], C.F.M. Sier[3], J.C.H. Hardwick[1], A.B. Nixon[2], C.P. Theuer[4], M.F. Fransen[5]*, L.J.A.C. Hawinkels[1]*

*contributed equally

Leiden University Medical Center, Departments of [1] Gastroenterology and Hepatology, [3] Surgery, [5] Immunohematology and blood transfusion, Leiden, the Netherlands
[2] Department of Medicine, Duke University Medical Center, Durham, NC, USA
[4] Tracon Pharmaceuticals, San Diego, CA, USA

ABSTRACT

Endoglin is a coreceptor for Transforming Growth factor (TGF)-β ligands that is highly expressed on proliferating endothelial cells and other cells in the tumor microenvironment (TME). Clinical studies have noted increased programmed cell death (PD)1 expression on cytotoxic T-cells in the peripheral blood of cancer patients treated with TRC105, an endoglin targeting antibody. In the current study we investigated the combination of endoglin antibodies (TRC105 and M1043) with an anti-PD1 antibody in four preclinical mouse models representing different stages of cancer development. In all models, the combination of endoglin antibody and PD1 inhibition produced durable tumor responses, leading to complete regressions in 30-40% of the mice. These effects were dependent on the presence of Fc-y receptors, indicating the involvement of antibody-dependent cytotoxic responses and the presence of CD8+ cytotoxic T cells. Interestingly, treatment with the endoglin antibody TRC105 significantly decreased the number of intratumoral regulatory T cells (Tregs). Endoglin expressing Tregs were also detected in human colorectal cancer specimens. Taken together these data provide a rationale for combining TRC105 and anti-PD1 therapy and provide additional evidence of endoglin's immunomodulatory role.

Keywords
Endoglin, TRC105, TGFbeta, tumor microenvironment, PD1, Tregs

INTRODUCTION

The tumor microenvironment (TME) is composed mainly of cancer-associated fibroblasts (CAFs), infiltrating immune cells and blood vessels, which are partly enveloped by pericytes. Endothelial cells in the newly formed blood vessels in the TME highly express the transforming growth factor (TGF)-β co-receptor endoglin, which has been correlated with poor prognosis and metastatic disease in many solid tumors [1, 2]. Upon stimulation with ligands, including bone morphogenetic protein (BMP) and TGF-β, endoglin promotes endothelial cell proliferation and migration, via signaling through phosphorylation of the SMAD-1 signaling molecule. In previous work, we and others demonstrated that endoglin is also expressed on CAFs, in particular at the invasive margin of colorectal tumors [3] and on mononuclear cells including lymphocytes and activated macrophages [4, 5].

TRC105 (Carotuximab, Tracon Pharmaceuticals, Inc.) is a humanized IgG1 endoglin neutralizing antibody, which has been studied in multiple clinical trials in oncology and age-related macular degeneration (AMD). In pre-clinical cancer models, we and others have shown that treatment with TRC105 inhibits angiogenesis, tumor growth and metastases [6-10]. Notably, TRC105 treatment might engage antibody dependent cellular cytotoxicity (ADCC) [11] and is more potent in immunocompetent mice compared to immunodeficient mice, indicating the active involvement of the immune system [7]. TRC105 binds to human endoglin with high avidity and inhibits BMP9 binding, but binds much less avidly to mouse endoglin, with consequently less inhibition of murine BMP9 binding. Therefore, a mouse-specific endoglin targeting rat IgG1 antibody, M1043, has been developed for pre-clinical studies. This antibody efficiently inhibits BMP9 induced endoglin signaling in mice [12].

Program cell death receptor 1 (PD1/CD279) is an immune checkpoint molecule which plays an important role in preventing self-reactive T-cell responses [13]. The PD1 ligands PD-L1 and PD-L2 are found on tumor cells, fibroblasts, and myeloid cells [14]. Inhibition of PD1 re-activates the tumor immune responses and PD1 antibodies have been approved for the treatment of melanoma [15], non-small cell lung cancer [16], renal cell carcinoma [17]. Additionally, anti-PD1 therapy has been approved for cancer patients with high microsatellite instability (MSI-H) representing the first tissue agnostic companion diagnostic approved by the FDA. In clinical trials, treatment with TRC105 increased PD1 expression on CD8+ T-cells in the blood of cancer patients [18]. Since the effects of TRC105 have been described to be immune-dependent and PD1 expression is increased upon TRC105 treatment, we hypothesized that a combination of TRC105 with anti-PD1 antibody therapy might enhance therapeutic responses.

In this study, we evaluated the effects of endoglin targeting antibodies in combination with a PD1 antibody in mouse models representing different cancer stages. We

compared the efficiency and mechanism of antibodies binding to human and mouse endoglin (TCR105 and M1043, respectively), and investigated the effects of combination treatment. Our data show enhanced therapeutic effects when combining endoglin antibodies with PD1 inhibitors, resulting in prolonged anti-tumor responses which are dependent on ADCC and CD8+ cytotoxic T-cells. Moreover, we present evidence that targeting endoglin-expressing regulatory T-cells in the TME reactivates the immunosuppressed tumor microenvironment.

MATERIALS AND METHODS

Cell culture

The C57BL/6 murine colon adenocarcinoma cell line MC38 and a BALB/c CT26, which stably expresses a codon optimized luciferase construct [3], were routinely cultured in DMEM/ F12 Glutamax with 10mM HEPES, 50µg/ml gentamicin, 100IU/ml Penicillin and 100µg/ml Streptomycin (Invitrogen, Landsmeer, NL), supplemented with 10% fetal calf serum (FCS) (Gibco, ThermoFisher Scientific, Waltham, MA, USA). Cells were tested directly before *in-vivo* use for mycoplasma contamination by PCR analysis.

Mice

In this study, 8 to 10 weeks old male C57BL/6 or BALB/c mice (Jackson Laboratories, Bar Harbor, Maine, USA) were used. Mice were maintained at the central animal facility at the Leiden University Medical Centre under standard conditions. All mice were treated twice a week with intraperitoneal (IP) injections of 10mg/kg bodyweight M1043 or 15mg/kg bodyweight TRC105 (both kindly supplied by TRACON Pharmaceuticals, San Diego, CA, USA) or a human IgG control (inVivoMAB, BioXcell, West Lebanon, NH, USA). For the combination studies, mice were additionally treated twice a week with either an anti-PD1 (clone J43, 10mg/kg body weight, IP injection) or a hamster IgG control (both inVivoMAB, BioXcell, West Lebanon, NH, USA). To investigate the FcReceptor interactions we investigated the therapeutic efficacy of TRC105 and TRC105 in combination with PD1 in an FcRI/II/III/IV KO mice [19] as described above. CD8 and CD4 dependent effects were studied using 200ug CD8 depleting antibody and 50ug for CD4 depletion (anti-CD8 Clone 2.42 and anti-CD4 clone GK1.5 in house production followed by potein G column purification) given one day prior to the therapeutic antibodies CD8 and CD4 depletion was checked using flow cytometry of the blood samples the day of treatment. The depleting antibody was given once a week during the entire experiment.

In order to investigate the tumor growth and survival, mice were subcutaneously injected with 250.000 MC38 or CT26 tumor cells. When palpable tumors were present treatment was started as described above and tumor volume was assessed by

caliper measurement. Mice were sacrificed when tumors reached 1500 mm^3. To investigate changes in the tumor immune infiltrate a short-term experiment was performed. Mice were subcutaneously injected with 250.000 tumor cells and when tumors were 5x5x5 mm therapy was started. Ten days after start treatment, when tumor sizes were still comparable, mice were sacrificed and after cardiac injection with 2 mM EDTA (Merck, Darmstadt, Germany) to eliminate the blood from the vessels, the tumors were collected and processed for histology, flow cytometry, RNA and protein isolation. For the M1043 studies in subcutaneous MC38 mice a total of forty female 6 to 8 week-old C57BL/6J mice were inoculated subcutaneously with $2.5x10^5$ CEA2 expressing MC38 colon carcinoma cells [20]. Once tumors reached 100 mm^3, mice were randomized into four treatment groups: 1) Isotype control (rat IgG2a, clone 2A3, Catalog # BE0089, BioXcell, West Lebanon, NH, USA); 2) 5 mg/kg M1043 (provided by Tracon Pharma, San Diego, CA, USA); 3) Anti-mouse PD1 antibody (RMP1-14, catalog # BE0146, BioXcell) at fixed dose of 150 g per mouse; and 4) Combination of M1043 and anti-PD1 antibodies at the aforementioned doses. Drugs were injected intraperitoneally every two days and tumor sizes monitored. When tumors reached 2000mm^3, mice were sacrificed according to institutional animal use guidelines (Duke University).

For imaging, mice were injected intravenously (iv) with 0.1mg TRC105 labeled with a near-infrared fluorescent dye 800CW according to the manufacturer (LI-COR Biosciences, Lincoln, Ne, USA). Mice were imaged using the Pearl Impulse Small Animal Imager (LI-COR Biosciences, Lincoln, Ne, USA) 24- and 48-hours post-injection, after which mice were sacrificed. Finally, tumors were also imaged *ex-vivo*.

For the orthotopic implantation, subcutaneous tumors were grown and upon reaching 0.5 cm^3 mice were sacrificed, and the donor tumor were divided in 1-2 mm^3 pieces. These pieces were transplanted to the caecum wall of a recipient mice [21] In short, mice were sedated using isoflurane followed by a small incision in the center of the abdomen. The caecum was isolated and a small piece of tumor (1x1x1mm) was attached to the caecal wall, followed by the closure of the peritoneal wall and skin. Bioluminescent imaging was performed as described before. In short mice received an IP injection with 100mg/kg luciferin (D-luciferin sodium salt, Synchem, Altenburg, Germany) and were subsequently imaged on the IVIS lumina-II (Perkin Elmer, Waltham, USA) signal. The signal was quantified using the living image software. Eight days post-transplantation mice were randomized based on equal bioluminescent signal after which treatment was started. Thirty-six days after transplantation mice were, imaged, sacrificed and the tumor volume was measured using a caliper.

To investigate early stages of cancer development, the Azoxymethane (AOM) Dextran Sodium Sulphate Sodium (DSS) colitis-associated cancer model was used. Wildtype C57/Bl6 jico mice received one IP injection with 10mg/kg azoxymethane (Sigma, Zwijndrecht, the Netherlands), which induces aberrant DNA methylations in the

colon and liver [22]. In order to accelerate tumor formation, mice were subsequently exposed to three, 7-day cycles of 1,5% DSS (MP Biomedicals, Santa Ana, CA, USA) supplied in the drinking water with 2week intervals. Mouse weights were monitored every other day. In previous studies we observed small colonic lesions 48 days after AOM injections. Therefore, therapy was started at this time point. At the end of the experiment (84 days) mice were sacrificed by cervical dislocation and colons and livers were obtained. The number of colonic lesions was counted and one lesion per mouse was used for flow cytometric analysis. The remaining material was fixed in 4% buffered formaldehyde (Added Pharma, Oss, The Netherlands) and embedded in paraffin (Leica Biosystems, Richmond, IL, USA).

Flow cytometry

Tumors were mechanically disrupted and incubated for 15 minutes at 37°C in DMEM containing 1mg/ml liberase TL (Roche, Woerden, The Netherlands). Single-cell suspensions were prepared by mincing the tumors through a 70-µm cell strainer (BD Bioscience, Breda, the Netherlands). For cell surface staining, cells were resuspended in FACS buffer (PBS + 0.5% bovine serum albumin (BSA Sigma, Zwijndrecht, The Netherlands) + 0.05% sodium azide (pharmacy, Leiden University Medical Center). Cells were stained with Life death UV marker, specific antibodies indicated in supplementary table 1 (mouse) and -2 (human) or MC38 specific tetramers (kindly provided by Kees Franken department of Immunohematology and Blood Transfusion, LUMC) for 1 hour. After incubation cells were washed 3 times with FACS buffer and analyzed on an LSRII (BD Bioscience, Breda, the Netherlands). For the FoxP3 staining, the eBioscience Foxp3/Transcription Factor staining buffer set was used according to the one-step protocol for intranuclear proteins. Data analyses were performed using Flowjo 10.0.6 (Flowjo, data analysis software, Ashland, OR, USA).

Histology

Four µm sequential sections were deparaffinized and stained with hematoxylin and Eosin (HE) or processed for immunohistochemistry as described before [10]. In short sections were deparaffinized, blocked in 0.3% hydrogen peroxidase (H_2O_2, Merck, Darmstadt, Germany) in methanol for 20 minutes. Next slides were rehydrated, and antigen retrieval was performed by boiling in 0.01M sodium citrate pH6.0 for 10 minutes. Slides were washed and incubated with primary antibodies against CD31 (1:1600, Santa Cruz, Dallas, TA, USA), α- smooth muscle actin (SMA) (1:1600, Progen, Heidelberg, Germany), endoglin (1:100, R&D systems Minneapolis, MN, USA) Foxp3 (1:25, Thermo fisher, Bleiswijk, the Netherlands) diluted in 1% PBS/BSA) overnight at room temperature in a humidified box. The next day slides were incubated with appropriate biotinylated secondary antibodies (DAKO, Glostrup, Denmark) or anti-

Goat-alexa488 (Abcam) and anti-Rat-alexa568 (Invitrogen) for immunofluorescent staining slides were mounted with prolong gold anti fade (Thermo fisher) including DAPI. For IHC slides were incubated for 30 minutes at room temperature using Vectastain complex (Vector Labs, Burlingame, CA, USA). Slides and color developed with the DAB+ reagent (DAKO, Glostrup, Denmark) for 10 minutes. Nuclei were counterstained with Mayers Haematoxylin (Merck, Darmstadt, Germany) and slides were rinsed in tap water , dehydrated and mounted using Entellan (Merck, Darmstadt, Germany). Finally, pictures were taken with an Olympus BX51 light microscope equipped with an Olympus DP25 camera using the program CellSense and analyzed using ImageJ. For confocal microscopy LICA SP8 Lightning was used and pictures were processed using LICA LAS-X software.

Statistical analysis

Statistical analysis was performed using GraphPad/Prism software, version 7.0 (Graphpad Prism Software, Inc. La Jolla, CA, USA) All data are presented as mean +/- standard deviation unless otherwise indicated. Differences in survival were assessed by the Log-rank/Mantel-Cox test. For all others when normally distributed, Students t-test, and ANOVA or Kruskal-Wallis (non parametric) were used to test for significant differences, as indicated in the figure legends. P-values <0.05 were considered statistically significant.

Ethical approvals

All experiments using human material were performed according to the code of conduct for responsible use of human tissue and medical research as drawn up by the federation of the Dutch medical societies in 2011, guidelines of medical ethical committee of the LUMC and conducted in accordance to the declaration of Helsinki.

All animal experiments were approved by the national Dutch animal ethics committee under project license number AVD116002017858 and AVD11600201571 and accordance with rules and regulation of the animal welfare body of the LUMC. Animal experiments conducted at Duke University were performed in the Duke Preclinical Translational Research Unit in accordance with the Institutional Animal Care and Use Committee (IACUC) of Duke University and Duke University Medical Center.

RESULTS

Combined endoglin/PD1 targeting reduces tumor burden in a chemically induced colorectal cancer model

To investigate if endoglin targeting can decrease tumor burden in early stage colorectal tumor development and if therapeutic effects can be enhanced together with checkpoint inhibition, we employed an azoxymethane (AOM) dextran sulfate sodium (DSS) colitis-associated cancer model. These mice show high-grade adenomas with dysplasia, but without invasion through the basement membrane (Supplementary figure 1A/B/C). Mice were either treated with endoglin antibody (TRC105 or M1043) and/or PD1 antibody or appropriate IgG controls starting at day 48 after AOM injection. At the end of the experiment (day 84) mice were sacrificed and the number of colonic lesions was counted. Treatment with TRC105 significantly reduced the number of lesions compared to control, which was further reduced by combination with a PD1 antibody (Figure 1A/B). The size of the remaining lesions was also significantly reduced by the TRC105/PD1 combination compared to IgG controls (Figure 1C). Since TRC105 binds to mouse endoglin with low affinity, we also used M1043, a specific mouse endoglin neutralizing antibody. In contrast to TRC105, M1043 monotherapy did not reduce the number of lesions in this experiment, although the combination with PD1 was highly effective in reducing the lesion count and size (Figure 1 D/E/F). Taken together these data show that targeting endoglin by using TRC105 can reduce tumor burden in an early stage tumor model and that these effects can be enhanced by combining endoglin and PD1 targeting antibodies.

TRC105/anti-PD1 therapy inhibits orthotopic MC38 tumor growth

To investigate the effects of combination therapy in a more advanced cancer model, we used a MC38 syngeneic orthotopic transplantation model. In short, part of a subcutaneously grown MC38 tumor, expressing codon-optimized luciferase, was transplanted onto the caecal wall of recipient mice (Supplementary figure 2A). Bioluminescent imaging was performed at day 8 after tumor transplantation, after which mice were allocated into treatment groups based on equal bioluminescent signal (Supplementary figure 2B). Tumor specific T-cell effects were assessed at day 17 (9 days after start treatment) by flow cytometry for the MC38 specific neo-epitopes ADPGK and DPAGT-1 tetramers [23], (gating strategy in Supplementary figure 2C). CD8+ DPAGT-1 positive cells increased slightly in the TRC105, PD1, and combination-treated mice compared to controls. M1043 alone did not induce tumor specific T-cells (Supplementary Fig 2D). A similar trend was present in ADPGK recognizing CD8 T-cells, but did not reach statistical significance (Supplementary figure 2E). At the end of the experiment (36 days post tumor transplantation) mice were sacrificed

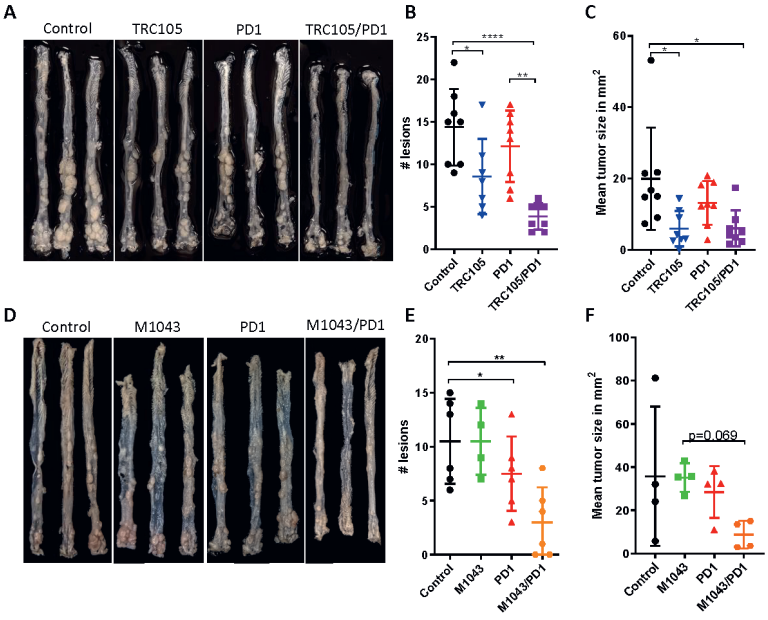

Figure 1. Combined endoglin/PD1 targeting reduces tumor burden in a chemically induced colon cancer model. Azoxymethane (AOM)/dextran sodium sulphate (DSS) model to study early colon tumor development. From day 48 on mice were treated twice weekly with anti-endoglin antibodies or control IgG and twice a week with anti PD-1 or IgG control until day 84 when mice were sacrificed. **A.** Images obtained from the mouse colon at the end of the experiment (84 days) showing multiple lesions in the distal colon. B. Quantification of the number of colonic lesions upon treatment with control IgG, anti-PD1, anti-endoglin (TRC105), and the TRC105/PD1 combination. Combination treated mice show significantly reduced tumor formation compared to monotherapy and IgG controls (one way ANOVA). C. Tumor volume measurements showing significantly smaller tumors in the combination treated mice (Kruskal-Willis test for multiple comparison). D. Images obtained from the distal mouse colon at the end of the experiment showing multiple lesions. E. Quantification of the number of lesions showing a significant decrease in the combination group (M1043/PD-1) compared to the IgG controls (one way ANOVA). F. Tumor volume measurement of the colonic lesions (Kruskal-Willis test for multiple comparison). Data shown are representative from two or more independent experiments with 6-8 mice per group. * P≤0.05 ** P<0.01 **** P<0.0001.

and the tumor volume was determined by caliper measurements. In contrast to M1043, TRC105 and PD1 antibody monotherapy and the combination of M1043 and PD1 antibody treatment resulted in reduced tumor volume compared to control IgG. Strikingly, the combination of TRC105 and PD1 antibody resulted in a more profound reduction of the tumor volume by bioluminescent imaging and caliper measurements (Figure 2A/B). Remaining tumors were processed for histological analysis and stained for H&E, the pan-endothelial marker CD31 (Figure 2A, middle panel) and endoglin (Figure 2A, right panel), using an antibody recognizing a non-overlapping endoglin epitope. No significant differences were detected in the number of CD31 or endoglin expressing blood vessels (Figure 2C/D) in the remaining tumors. Of note, vessel density could not be assessed in mice with complete tumor regressions and differences in tumor size were not considered in the analysis.

Combined, these data indicate that TRC105/PD1 antibody therapy induced marked anti-tumor responses in an orthotopic MC38 colon cancer model and TRC105 seemed more effective in tumor inhibition compared to M1043 therapy.

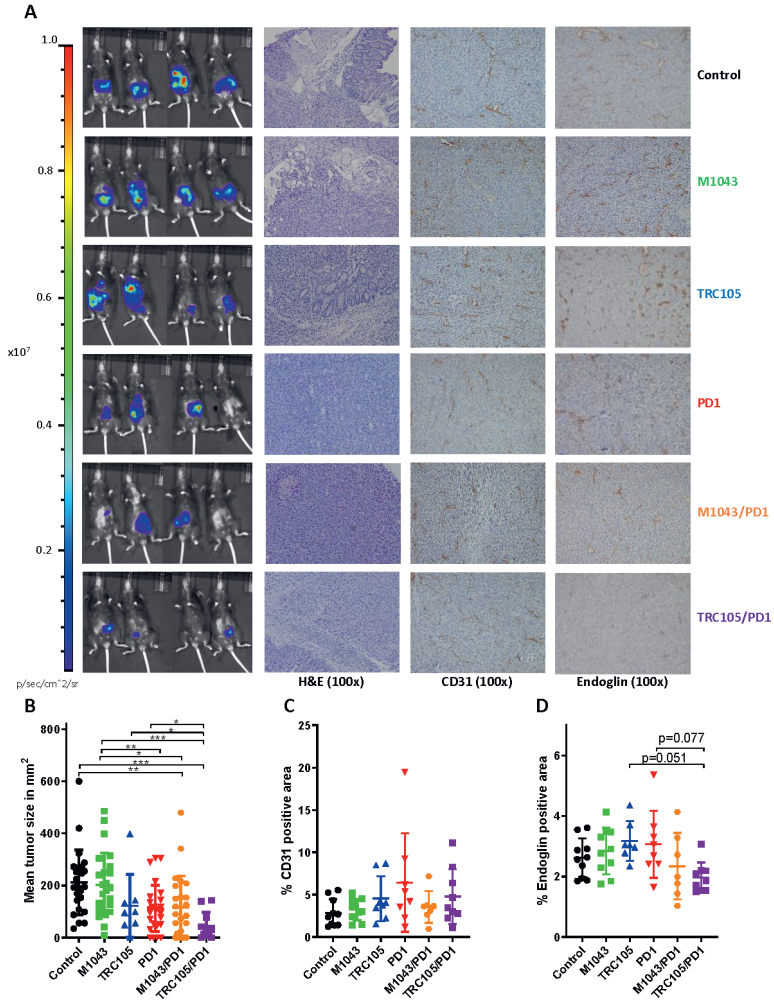

Figure 2. Endoglin/PD-1 therapy inhibits orthotopic tumor growth. Tumors were orthotopically transplanted in recipient mice and after engraftment and randomization, mice were treated twice a week with anti-endogin or control IgG and twice a week with anti PD-1 or IgG control. **A**. Bioluminescent imaging (left panel) at the end of the experiment showing anti-tumor responses. The right panel shows (immuno) histochemical analysis for H&E, CD31 and endoglin. **B.** Quantification of the tumor volume at the end of the experiment showing significantly smaller tumors upon combination therapy, especially in the TRC105/PD-1 group. Data are from 2 independent experiments with 8-20 mice per group (one way ANOVA) **C.** Quantification of tumor CD31 staining showing no significant difference in the number of CD31 positive cells (Kruskal-Willis test for multiple comparison) **D.** Quantification of intratumoral endoglin staining showing no significant differences between treatment groups. Quantifications are from at least two independent experiments (one way ANOVA). * P≤0.05 ** P<0.01 *** P<0.001.

TCR105/PD1 therapy efficiently reduces tumor growth and induces memory anti-tumor responses

In order to assess the immune responses in more detail, we evaluated the therapeutic effectivity of the mouse endoglin antibody M1043 with PD1 antibody in a subcutaneous MC38 model. A significant delay in tumor outgrowth was observed in the combination therapy treated mice and resulting complete tumor regression in 20% of the mice in the combination therapy group (Figure 3A and Supplementary figure 3A). Given the fact that TRC105 binds murine endoglin with lower avidity, we confirmed that TRC105 can still bind to mouse endoglin and accumulates in subcutaneous mouse tumors. Therefore we labelled TRC105 with the near-infrared dye CW800. Upon intravenous injection in mice bearing subcutaneous MC38 tumors, tumor accumulation of TRC105 was observed 24h and 48h post injection as well as *ex vivo* (Figure 3B).

The subcutaneous MC38 model was used to directly compare the efficiency of M1043 and TRC105 versus an isotype control. These data demonstrate significantly more therapeutic efficacy of TRC105 compared to M1043 (Supplementary figure 3B). Therefore, we focused further studies on TRC105/PD1 only. The therapeutic benefit of TRC105/PD1 antibody therapy was assessed in MC38 and CT26 subcutaneous tumor models in C57BL/6 and Balb/c mice, respectively. TRC105 or PD1 antibody monotherapy delayed tumor growth and prolonged survival, but effects were more pronounced in animals who received TRC105/PD1 combination therapy in both the MC38 (Figure 3C) and CT26 model (Figure 3D). Complete tumor responses were observed in 30-40% of the mice in both models. To investigate memory anti-tumor responses, the surviving, tumor-free mice were injected again with $2.5*10^5$ MC38 or $2.5*10^5$ CT26 cells 60 days after the initial tumor cell injection. Importantly, no tumor outgrowth was observed after re-challenge with tumor cells, implying that a memory anti-tumor response was induced. Our data show that combined TRC105/PD1 antibody therapy delays tumor growth compared to either antibody alone, induces complete and sustained regression in both the MC38 and CT26 subcutaneous tumor models, and prevents tumor growth after re-challenge with tumor cells.

TRC105/PD1 antibody therapeutic effects are ADCC dependent

We next investigated the underlying mechanism for the activity of the TRC105/PD1 antibody combination. TRC105 can mediate ADCC, which requires binding to Fc-receptors. We therefore investigated whether the TRC105 and TRC105/PD1 antibody effects were dependent on Fc-receptor binding in $FcγR^{KO}$ mice. MC38 bearing C57Bl6 and $FcγR^{KO}$ mice injected with human IgG showed similar tumor outgrowth and survival (supplementary figure 3C). Notably, the activity of TRC105 and TRC105/PD1 combination therapy was completely abolished in $FcγR^{KO}$ mice (Figure 3E/F) indicating, that the therapeutic effects of TRC105 and the TRC105/PD1 combination are dependent on Fcγ receptor binding *in vivo*.

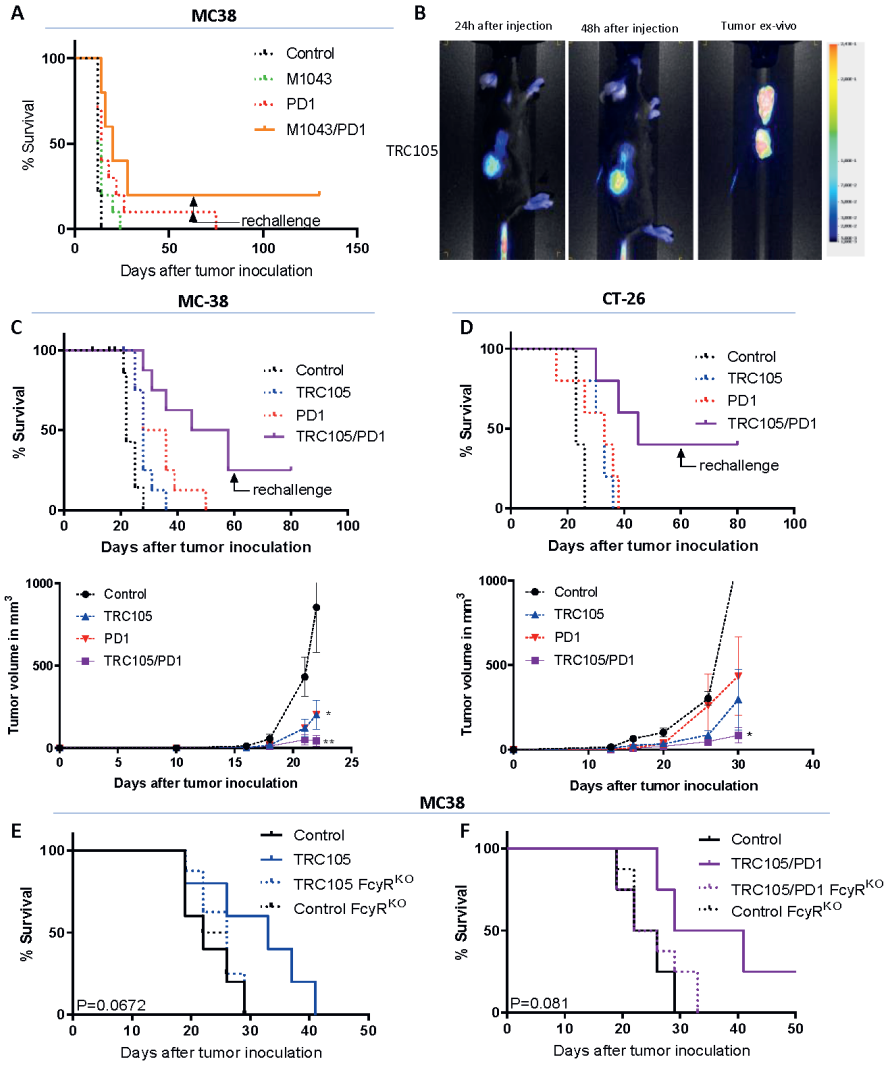

Figure 3. TRC105/PD-1 therapy efficiently reduces tumor growth, induces memory T cell responses and is dependent on FcyR expression. When tumors were palpable mice were treated twice a week with anti-endoglin or control IgG and twice a week with anti PD-1 or IgG control **A.** A combination of M1043 and PD1 results in significantly improved mouse survival and induced memory T cell responses, since rechallenge with tumor cells does not result in tumor outgrowth. **B.** Intravenously administered, CW800 labeled TRC105 shows high tumor accumulation in subcutaneous MC38 tumors (representative image from 2 mice). **C.** Combination treatment with TRC105/PD1 significantly increases survival of mice bearing MC38 (n=7-8 mice per group) or (**D**) CT26 subcutaneous tumors (n=5 mice per group). **E.** Therapeutic effects of TRC105 or combination therapy (**F**) are diminished in a FcyRI,II,III,IV KO mouse, indicating the involvement of ADCC (n=5-8 mice per group). Statistical analysis includes Log-rank/Mantel-Cox test for survival analyses, one way ANOVA for multiple comparison on day 22 for C and day 30 for D. * P≤0.05 ** P<0.01.

TRC105/PD1 therapy requires T cell infiltration and activity

Next, we assessed changes in immune cell infiltrate upon combination treatment. Subcutaneous MC38 tumors of similar size (Supplementary figure 4A) nine days after start of treatment were evaluated to exclude potential effects of tumor volume on the composition of the immune infiltrate. Immunohistochemistry showed decreased numbers of Ki67+ proliferating cells, accompanied by increased numbers of apoptotic, cleaved caspase-3 positive cells (Supplementary figure 4B), indicating anti-tumor responses. The number of endoglin-positive blood vessels was unaffected at this time point (Supplementary figure 4C). Treatment with TRC105 or the combination of TRC105/PD1 antibody increased the number of intratumoral CD8+ T cells (Figure 4A). Moreover, we observed a significant increase in the number of activated, granzyme B+/CD8+ T cells upon TRC105 or PD1 or TRC105/PD1 antibody combination therapy in the circulation (Figure 4B). Activation of T cells was further confirmed by mRNA expression analysis of the tumor tissue, showing that granzyme B mRNA expression was particularly increased following TRC105/PD1 antibody combination treatment (Figure 4C and 4D). Increased numbers of tumor infiltrating CD8+ T cells was confirmed by immunohistochemical analysis (Figure 4E). Protein levels of VEGF, INF-y and TGFβ-1 within the tumor lysates did not differ although levels varied considerably between and within groups (supplementary figure 4E). Taken together these data indicate that an increased number of CD8+ T cells were recruited and activated upon TRC105/PD1 combination therapy.

To further investigate if CD8+ T cells are instrumental for the therapeutic responses, MC38 cells were subcutaneously injected in mice and a CD8+ depleting antibody was given before the initiation of TRC105 or TRC105/PD1 antibody treatment. This resulted in a significantly reduced number of circulating CD8+ T cells (supplementary figure 4F) in these groups. In T cell depleted mice, therapeutic responses induced by TRC105 or TRC105/PD1 antibody combination were abolished compared to control IgG treated, mice (Figure 4 F/G). These data suggest that the therapeutic effect of combination therapy is dependent on the activity of CD8+ T cells and involves their recruitment and activation.

Targeting of FOXP3 immune subsets by endoglin targeted therapy

On the ninth day, subcutaneous MC38 tumor experiments anti-endoglin therapy did not cause significant differences in the number of peripheral blood $Treg^{CD4+CD25+Foxp3+}$cells pre- and post- treatment or between the treatment groups (Figure 5A). However, we observed a significantly decreased percentage of regulatory T cells in the tumor in the TRC105 and TRC105/PD1 antibody treated mice, compared to the control IgG and PD1 antibody monotherapy treated mice (Figure 5B). Moreover, the CD8+/Treg ratio significantly increased to a more beneficial ratio to reach anti-tumor effects in the combination therapy treated mice (Figure 5C). A

striking increase in endoglin expression on tumor localized Tregs was present, compared to circulating Tregs in these mice (Figure 5D). Endoglin expression was present only on a subpopulation of Tregs within the tumor and not on conventional CD4+ T cells (Figure 5E). Treatment with TRC105 significantly reduced the number of intratumoral CD25+/Foxp3+ cells (Figure 5F).

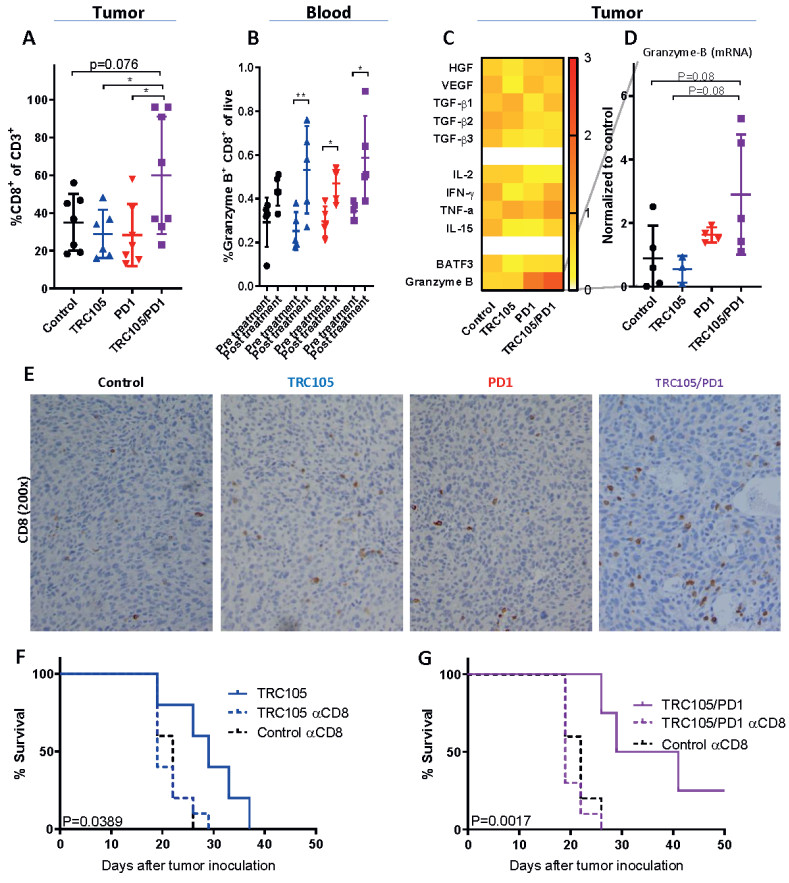

Figure 4. TRC105/PD-1 therapy requires CD8+ T-cell infiltration. When tumors were palpable mice were treated twice a week with anti-endoglin or control IgG and twice a week with anti PD-1 or IgG control. After 9 days of treatment mice were sacrificed and the immune infiltrate was examined **A.** Upon treatment with TRC105/PD1 combination therapy the percentage of intratumoral CD8+ T cells is increased (mean of 2 independent experiments, n=4 mice per group per experiment, one way ANOVA). **B.** Increased number of circulating granzyme B+ CD8+ T cells post-treatment (n=3-5 mice per group, paired t-test). **C.** Heatmap showing mRNA expression of growth factors and genes involved in immune regulation, normalized to control IgG treated mice (n=3-5 mice per group). Increased granzyme B expression within the tumor in combination therapy treated mice is observed (**D**) **E.** Immunostaining revealing increased CD8+ T cells throughout the tumors upon treatment with TRC105/PD-1 (one way ANOVA). The therapeutic effects of TRC105 monotherapy (**F**) and combination therapy (**G**) were completely depending on CD8+ T cells (n=5 (control)-10 (CD8 depleted) mice per group, Log-rank/Mantel-Cox test). * P≤0.05 ** P<0.01.

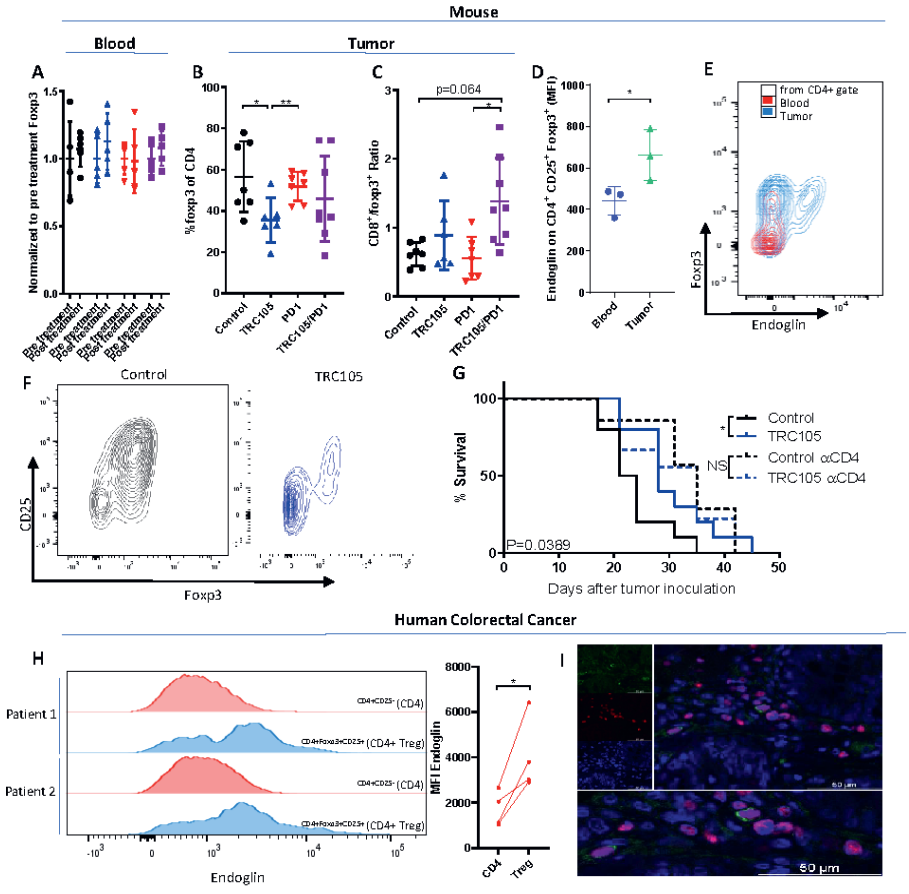

Figure 5. Endoglin expressing FoxP3 cells are detected intratumorally and are targeted by anti-endoglin therapy. A. The number of FoxP3 cells in the circulation of tumor bearing mice did not change pre- and post- treatment (n=5 mice per group, paired t-test). **B.** A significant decrease in intratumoral Tregs (FoxP3+CD25+CD4+) was observed (one-way ANOVA), resulting in increased CD8/FoxP3 tumor ratios (**C**, mean of 2 independent experiments, n=4 mice per group per experiment, Kruskal-Willis test for multiple comparison). **D/E**. FACS analysis revealed higher endoglin expression on intratumoral FoxP3 cells, compared circulating FoxP3 cells from the same mouse (mean fluorescent intensity, n=3 mice per group, t-test). **F.** Flow cytometry plot of TRC105 treated MC38 tumors, showing a decrease in CD25+/Foxp3+ cells upon TRC105 treatment. **G.** TRC105 significantly enhances survival of mice bearing MC38 tumors (p=0.039), which is lost upon depletion of CD4+ cells (p=0.039 vs p=0.37 respectively, n=7-10 mice per group, Log-rank/Mantel-Cox test). **H.** In human colorectal cancer samples endoglin expression on intratumoral Tregs was observed by flow cytometry analysis (representative image from n=4 patients, paired t-test). **I.** Immunohistochemical analysis shows colocalization of endoglin (green) with FoxP3 (red) in a subset of FoxP3 cells in human CRC tissues (representative image from n=4 patients). * P≤0.05 ** P<0.01.

To further investigate the targeting of Foxp3+ Tregs we depleted CD4+ cells, compromising the Foxp3+ population. MC38 cells were subcutaneously injected in mice and a CD4+ depleting antibody was given before the initiation of TRC105 treatment. This resulted in a loss of circulating CD4+ T cells (supplementary figure

5C) in the depleted groups. Mice not showing CD4+cell depletion (indicated in red) were excluded from the experiment. In control mice TRC105 effectively delayed tumor growth (p=0.039) as shown before. However, the therapeutic effects of TRC105 are lost once the CD4+ T cells were depleted (Figure 5G, p=0.37). These data suggest that therapeutic TRC105 effects are CD4 cell dependent and most probably involves targeting endoglin expressing Foxp3+/CD4+ cells.

Finally to illustrate the potential translational relevance of our findings, we investigated whether endoglin is also expressed on Tregs in a limited number of human colorectal cancer tissues by using flow cytometry. High endoglin expression was seen on a subset of Tregs$^{CD4+CD25+Foxp3+}$ compared to the CD4+$^{CD25-Foxp3-}$ population within the tumor (Figure 5H). To confirm our flow cytometry findings, we performed immunofluorescent double staining for endoglin and Foxp3 on colorectal cancer tissue sections (Figure 5I). These data revealed high endoglin expression of a subset of intratumoral Tregs. Taken together, our data confirm that a subset of Foxp3 cells co-express endoglin in mouse colorectal tumors and can also be detected in human CRC.

DISCUSSION

In this study, we demonstrated that combined therapy with anti-endoglin and anti-PD1 antibodies significantly increases the therapeutic efficacy in several pre-clinical cancer models, including subcutaneous, orthotopic, and chemically induced colorectal cancer models. The endoglin antibody TRC105 acted principally via immune dependent mechanisms, where both CD8. the Fc receptors played instrumental roles in the therapeutic response. In addition we identified endoglin expressing Tregs in mouse and human colorectal cancer tissue, which also seem to be targeted by TRC105, as the effects are lost when CD4+ cells are depleted.

TRC105 was initially described in the late 1990s [8, 9], and subsequently has been studied in Phase 2 and Phase 3 clinical trials. Since high endoglin expression has been reported on angiogenic endothelial cells and endothelial endoglin expression has been linked to disease progression and prognosis [2], targeting endoglin seems a logical therapeutic approach in solid tumors. Indeed, we and others have shown that anti-endoglin therapy inhibits tumor growth and metastasis formation in various cancer models [6, 8-10, 24]. Furthermore, targeting the VEGF pathway activates alternative pathways, of which endoglin has been frequently reported [10, 25-27].

It was surprising that M1043 was less effective in reducing tumor growth in the presented tumor models. M1043 is a mouse-specific endoglin targeting antibody, which efficiently inhibits downstream BMP9 induced signaling [12] and supplementary figure 5), while TRC105 less effectively inhibits mouse BMP9 binding to endoglin. Rat IgG1 is, however not capable of inducing ADCC, compared to other isotypes,

making it an interesting approach to change the M1043 isotype to Mouse IgG2a, thereby creating an antibody which blocks ligand binding but also induces ADCC.
Fc-mediated effects have been clearly shown for human IgG subtypes and the human IgG1 antibody TRC105, which is able to bind mouse Fc-receptors [28]. Moreover FcR mediated ADCC appeared crucial for the mechanism of action of endoglin antibody in our tumor models. In humans, the TRC105 IgG isotype may bind with higher affinity to Fc Receptors compared to mouse Fc receptors, even further enhancing ADCC-responses. Previous studies have shown that the therapeutic PD1 antibody effects are independent on Fc receptor binding [29]. These data also indicate that evoking an immune response might be a more important mechanism of action for endoglin antibodies than inhibiting BMP9 binding.
In addition to endothelial cells, endoglin expression has been reported on (cancer-associated) fibroblasts in prostate cancer [30] and colorectal cancer [3]. Endoglin expression seems to be important for fibroblast survival *in-vitro* and stimulates metastatic dissemination [3]. Furthermore endoglin expression has also been described on macrophages, where it seems to be important for differentiation and phagocytosis [31]. In the current study we show that endoglin is expressed by regulatory T-cells, posing them as a novel target for endoglin targeted therapy. Although endoglin expression on CD4+ cells has also been observed by others [32-34], endoglin expression on Treg cells has only been described before in an *in-vitro* setting in which Tregs were cultured with adipose derived mesenchymal stromal cells [34]. Strikingly, we observed that endoglin expression on Tregs is significantly increased in tumor tissue compared to the peripheral circulation. Furthermore, we show that endoglin targeted therapy decreased the number of Tregs in tumors, thereby potentially contributing to the tumor responses. Depletion of Tregs within the tumor using antibody therapy has also been shown by others, for example using anti-CD25 [35] and anti-CTLA-4 antibodies [36] in mice. Since endoglin therapy targets multiple subsets of cells within the tumor microenvironment (i.e., proliferating endothelial cells, fibroblasts and Tregs), TRC105 may more efficiently inhibit tumor growth and metastasis compared to other anti-angiogenic therapies. The fact that endoglin expressing Tregs could be detected in colorectal cancer tissue might explain the data from a previous clinical trial showing a significantly decreased number of circulating Tregs upon TRC105 therapy [18]. Although we could not show a clear endoglin positive population in the blood of mice, we were able to detect endoglin expressing Tregs in the blood of healthy volunteers (data not shown).
In conclusion, in this study we show that combining endoglin with PD1 targeted therapy in four preclinical cancer models strongly increases therapeutic effects. We propose a model in which TRC105 binds to endoglin expressing endothelial cells, fibroblasts, and endoglin expressing Tregs within the tumor, evoking a FcR dependent ADCC response. Consequently, the increased recruitment and activity of CD8+ cells

evokes sustained tumor regression and produce a memory T cell response. Results from a phase 1b dose-escalation study of carotuximab (TRC105) in combination with nivolumab (anti-PD1) in patients with metastatic Non-Small Cell Lung Cancer (NCT03181308) should reveal if this combination strategy is effective in human patients.

Conflict of interest

This study was supported by a sponsored research agreement from TRACON Pharmaceuticals. C.P. Theuer has ownership interest (including patents) in TRACON Pharmaceuticals. No potential conflicts of interest were disclosed by the other authors.

Acknowledgments

This study was supported by a sponsored research grant from Tracon Pharmaceuticals to both Duke and Leiden University Medical Center, and research grants from Stichting Fonds Oncologie Holland (SFOH), and Stichting Sasha Swarttouw-Hijmans and Dutch Cancer Society (UL2014-6828). We would like to thank Dr. Sjef Verbeek for the FcR I,II,III,IV KO mice, Kees Franken for the MC38 specific tetramers. Finally, the authors would like to thank the Animal facility of the Leiden university medical center and the Duke Preclinical Translational Research Unit for facilitating the mice experiments.

Author contributions

MS performed experiments, designed and analyzed experiments and wrote the manuscript. MK, RA, BK, MT, YL, MP, LH, CS and MB performed and analyzed the experiments. AN, CT, CS, and JH revised the manuscript and provided critical feedback on experiments. LH and MF designed experiments, supervised the project and revised the manuscript.

All supplementary figures and tables are available online

REFERENCES

1. Saad, R.S., et al., *Endoglin (CD105) and vascular endothelial growth factor as prognostic markers in colorectal cancer.* Mod Pathol, 2004. **17**(2): p. 197-203.

2. Zhang, J., et al., *Prognostic value of endoglin-assessed microvessel density in cancer patients: a systematic review and meta-analysis.* Oncotarget, 2018. **9**(7): p. 7660-7671.

3. Paauwe, M., et al., *Endoglin Expression on Cancer-Associated Fibroblasts Regulates Invasion and Stimulates Colorectal Cancer Metastasis.* Clin Cancer Res, 2018. **24**(24): p. 6331-6344.

4. Lastres, P., et al., *Regulated expression on human macrophages of endoglin, an Arg-Gly-Asp-containing surface antigen.* Eur J Immunol, 1992. **22**(2): p. 393-7.

5. O'Connell, P.J., et al., *Endoglin: a 180-kD endothelial cell and macrophage restricted differentiation molecule.* Clin Exp Immunol, 1992. **90**(1): p. 154-9.

6. Takahashi, N., et al., *Antiangiogenic therapy of established tumors in human skin/severe combined immunodeficiency mouse chimeras by anti-endoglin (CD105) monoclonal antibodies, and synergy between anti-endoglin antibody and cyclophosphamide.* Cancer Res, 2001. **61**(21): p. 7846-54.

7. Tsujie, M., et al., *Anti-tumor activity of an anti-endoglin monoclonal antibody is enhanced in immunocompetent mice.* Int J Cancer, 2008. **122**(10): p. 2266-73.

8. Matsuno, F., et al., *Induction of lasting complete regression of preformed distinct solid tumors by targeting the tumor vasculature using two new anti-endoglin monoclonal antibodies.* Clin Cancer Res, 1999. **5**(2): p. 371-82.

9. Seon, B.K., et al., *Long-lasting complete inhibition of human solid tumors in SCID mice by targeting endothelial cells of tumor vasculature with antihuman endoglin immunotoxin.* Clin Cancer Res, 1997. **3**(7): p. 1031-44.

10. Paauwe, M., et al., *Endoglin targeting inhibits tumor angiogenesis and metastatic spread in breast cancer.* Oncogene, 2016. **35**(31): p. 4069-79.

11. Seon, B.K., et al., *Endoglin-targeted cancer therapy.* Curr Drug Deliv, 2011. **8**(1): p. 135-43.

12. Nolan-Stevaux, O., et al., *Endoglin requirement for BMP9 signaling in endothelial cells reveals new mechanism of action for selective anti-endoglin antibodies.* PLoS One, 2012. **7**(12): p. e50920.

13. Ishida, Y., et al., *Induced expression of PD-1, a novel member of the immunoglobulin gene superfamily, upon programmed cell death.* EMBO J, 1992. **11**(11): p. 3887-95.

14. Kleinovink, J.W., et al., *PD-L1 expression on malignant cells is no prerequisite for checkpoint therapy.* Oncoimmunology, 2017. **6**(4): p. e1294299.

15. Robert, C., et al., *Anti-programmed-death-receptor-1 treatment with pembrolizumab in ipilimumab-refractory advanced melanoma: a randomised dose-comparison cohort of a phase 1 trial.* Lancet, 2014. **384**(9948): p. 1109-17.

16. Garon, E.B., et al., *Pembrolizumab for the treatment of non-small-cell lung cancer.* N Engl J Med, 2015. **372**(21): p. 2018-28.

17. Motzer, R.J., et al., *Nivolumab for Metastatic Renal Cell Carcinoma: Results of a Randomized Phase II Trial.* J Clin Oncol, 2015. **33**(13): p. 1430-7.

18. Karzai, F.H., et al., *A phase I study of TRC105 anti-endoglin (CD105) antibody in metastatic castration-resistant prostate cancer.* BJU Int, 2015. **116**(4): p. 546-55.

19. Fransen, M.F., et al., *A Restricted Role for FcgammaR in the Regulation of Adaptive Immunity.* J Immunol, 2018. **200**(8): p. 2615-2626.

20. Hand, P.H., et al., *Evaluation of human carcinoembryonic-antigen (CEA)-transduced and non-transduced murine tumors as potential targets for anti-CEA therapies.* Cancer Immunol Immunother, 1993. **36**(2): p. 65-75.

21. Tseng, W., X. Leong, and E. Engleman, *Orthotopic mouse model of colorectal cancer.* J Vis Exp, 2007(10): p. 484.

22. De Robertis, M., et al., *The AOM/DSS murine model for the study of colon carcinogenesis: From pathways to diagnosis and therapy studies.* J Carcinog, 2011. **10**: p. 9.

23. Yadav, M., et al., *Predicting immunogenic tumour mutations by combining mass spectrometry and exome sequencing.* Nature, 2014. **515**(7528): p. 572-6.

24. Tabata, M., et al., *Antiangiogenic radioimmunotherapy of human solid tumors in SCID mice using (125)I-labeled anti-endoglin monoclonal antibodies.* Int J Cancer, 1999. **82**(5): p. 737-42.

25. Liu, Z., et al., *ENDOGLIN is dispensable for vasculogenesis, but required for vascular endothelial growth factor-induced angiogenesis.* PLoS One, 2014. **9**(1): p. e86273.

26. Liu, Y., et al., *Modulation of circulating protein biomarkers following TRC105 (anti-endoglin antibody) treatment in patients with advanced cancer.* Cancer Med, 2014. **3**(3): p. 580-91.

27. Liu, Y., et al., *Modulation of Circulating Protein Biomarkers in Cancer Patients Receiving Bevacizumab and the Anti-Endoglin Antibody, TRC105.* Mol Cancer Ther, 2018. **17**(10): p. 2248-2256.

28. Dekkers, G., et al., *Affinity of human IgG subclasses to mouse Fc gamma receptors.* MAbs, 2017. **9**(5): p. 767-773.

29. Dahan, R., et al., *FcgammaRs Modulate the Anti-tumor Activity of Antibodies Targeting the PD-1/PD-L1 Axis.* Cancer Cell, 2015. **28**(4): p. 543.

30. Romero, D., et al., *Endoglin regulates cancer-stromal cell interactions in prostate tumors.* Cancer Res, 2011. **71**(10): p. 3482-93.

31. Ojeda-Fernandez, L., et al., *Mice Lacking Endoglin in Macrophages Show an Impaired Immune Response.* PLoS Genet, 2016. **12**(3): p. e1005935.

32. Nowaczyk, R.M., et al., *Cells expressing CD4, CD8, MHCII and endoglin in the canine corpus luteum of pregnancy, and prepartum activation of the luteal TNFalpha system.* Theriogenology, 2017. **98**: p. 123-132.

33. Schmidt-Weber, C.B., et al., *TGF-{beta} signaling of human T cells is modulated by the ancillary TGF-{beta} receptor endoglin.* Int Immunol, 2005. **17**(7): p. 921-30.

34. Quaedackers, M.E., et al., *Cell contact interaction between adipose-derived stromal cells and allo-activated T lymphocytes.* Eur J Immunol, 2009. **39**(12): p. 3436-46.

35. Arce Vargas, F., et al., *Fc-Optimized Anti-CD25 Depletes Tumor-Infiltrating Regulatory T Cells and Synergizes with PD-1 Blockade to Eradicate Established Tumors.* Immunity, 2017. **46**(4): p. 577-586.

36. Tang, F., et al., *Anti-CTLA-4 antibodies in cancer immunotherapy: selective depletion of intratumoral regulatory T cells or checkpoint blockade?* Cell Biosci, 2018. **8**: p. 30.